



JAAS

An efficient method for high-precision potassium isotope analysis in carbonate materials

Journal:	<i>Journal of Analytical Atomic Spectrometry</i>
Manuscript ID	JA-ART-05-2022-000170.R2
Article Type:	Paper
Date Submitted by the Author:	09-Sep-2022
Complete List of Authors:	Wang, Xi-Kai; UNC-Chapel Hill, Earth, Marine and Environmental Sciences Liu, Xiao-Ming; UNC-Chapel Hill, Earth, Marine and Environmental Sciences CHEN, HENG; Lamont-Doherty Earth Observatory, Geochemistry Division

SCHOLARONE™
Manuscripts

1
2
3
4
5
6
7
8
9
10
11
12 **An efficient method for high-precision potassium isotope analysis in carbonate**
13 **materials**
14
15
16
17
18

19 **Xi-Kai Wang¹, Xiao-Ming Liu^{1*}, Heng Chen²**
20
21

- 22 **1. Department of Earth, Marine and Environmental Sciences, the**
23 **University of North Carolina at Chapel Hill, Chapel Hill, NC, 27599,**
24 **USA**
25
26
27
28
29 **2. Lamont-Doherty Earth Observatory, Columbia University, Palisades,**
30 **NY, 10964, USA**
31
32
33
34
35
36
37
38

39 *** Corresponding author: Xiao-Ming Liu (xiaomliu@unc.edu)**
40
41
42
43
44
45
46
47
48
49
50
51
52
53
54
55
56
57
58
59
60

Abstract

High-precision potassium isotope measurement in marine carbonates allows using this novel geochemical proxy to constrain seawater chemistry through geological time. However, these measurements are still scarce due to the challenges of low-K contents in carbonates during K ion chromatography, such as insufficient sample purification, non-quantitative yield, and high accumulative blank. Here we optimize a dual-column K purification method that addresses these challenges, achieving a satisfactory K separation using 100–150 mg carbonates for routine high-precision K isotope analysis on the Sapphire™ MC-ICP-MS. We then report K isotope compositions in multiple certified reference materials, including limestone, dolostone, coral, and basalt for future inter-laboratory comparisons. The optimized K purification method provides great potential for future K isotope studies of marine carbonates.

1. Introduction

Seawater composition reflects chemical exchanges between the lithosphere, hydrosphere, atmosphere, and biosphere.¹ Among all elements investigated, K and its stable isotopes (³⁹K and ⁴¹K) in seawater have been given particular attention, not only due to K being an essential nutrient for life,^{2–6} but also because K, a major cation in both Earth's crust (1.81%)⁷ and seawater (~400 µg/g)⁸, actively involves in various fluid-rock interactions between lithosphere and hydrosphere (e.g., silicate weathering^{9–13}; reverse weathering^{14–17}; hydrothermal alterations^{18–22}). Recent high-precision measurements of potassium isotopes (³⁹K and ⁴¹K) by multi-collector inductively coupled plasma mass spectrometer (MC-ICP-MS) have revealed significant ⁴¹K/³⁹K variations in terrestrial samples, and a significantly higher $\delta^{41}\text{K}$ value in seawater (~0.12 ‰)^{23,24} relative to the bulk silicate earth (BSE) (~-0.43 ‰)^{25,26}. This could be explained by seawater K isotope mass balance, where major K sources (riverine and hydrothermal inputs) and sinks (reverse weathering and oceanic basalt alteration) in the ocean have a distinct magnitude of fluxes and isotopic signatures^{11,24,27}. Therefore, records of the past K isotope composition in seawater should preserve information on how these sources and sinks change, providing key constraints on global K cycling over geological history.

Marine carbonates are one of the most important archives for seawater chemistry with regard to both elemental and isotopic compositions.^{28–31} However, to date, limited studies have been carried out to explore the K isotope behavior in marine carbonates.^{32,33} A major obstacle to such studies is that the K isotope analysis in carbonate materials requires an efficient and high-yield pretreatment step to separate K from other matrix elements. Although a growing number of studies have developed cation-exchange chromatographic protocols for quantitative K purification (**Table 1**), the application for marine carbonates is challenging due to their low-K contents and high matrices (e.g., Ca and Mg)^{27,34}. To obtain enough K (e.g., 1 µg) for the high-precision isotopic analysis, more than 100 mg of carbonates are typically needed.

1
2
3 For columns packed with resin volume less than 3 mL,^{35–39} this amount of loading exceeds their optimal
4 capacity (i.e., 10% of the total column capacity)^{40,41}, therefore resulting in potential K loss and
5 breakthroughs of matrix elements (e.g., Na, Mg, Ca) into K collections. Alternatively, using columns with
6 larger resin volume usually requires a larger volume of eluent (up to 300 mL),⁴² increasing total procedural
7 blanks. Furthermore, changes in both K amount and K/matrix ratio can shift elemental elution curves. For
8 example, Chen *et al.*⁴³ reported a dual-column K purification method for K-rich materials (i.e., silicate rocks,
9 soils, and sediments) with high loading capacity and acceptable procedural blanks, however, their protocol
10 cannot efficiently exclude excessive Mg from carbonates. Repetition of their columns will nevertheless
11 increase the accumulative blank. As such, a robust K chromatography suitable for low-K marine carbonates
12 with low blank and high yield is needed.
13
14
15
16
17
18

19
20 In this study, we present an efficient dual-column K purification protocol for marine carbonates to achieve
21 high-precision K isotope measurements using a SapphireTM MC-ICP-MS. The first column was modified
22 based on Chen *et al.*⁴³ through optimization of the K elution range under various amounts of carbonate
23 loading. The second column was developed using a synthetic solution, certified references, and carbonate
24 samples aiming for a better K separation. We tested the yield and procedural blank of the newly developed
25 K purification method, and we successfully applied this method to three well-studied carbonate references,
26 one dolostone sample, and one silicate standard.
27
28
29
30

31 **2. Experimental methods**

32 **2.1 Chemicals and samples**

33
34
35
36 Ultra-pure water with a resistivity of 18.2 MΩ was produced using a Milli-Q purification system (Direct-
37 Q[®] 3 UV, Merck MilliporeTM, Germany). Nitric acid (HNO₃), hydrochloric acid (HCl), and hydrofluoric
38 acid (HF) were distilled twice from ACS Grade using a SavillexTM DST-1000 still. Double-distilled HNO₃
39 and HCl were diluted with Milli-Q water to the required concentrations.
40
41
42

43 To optimize the K separation, we investigated three in-house carbonate samples: a limestone from Key
44 Largo, a dolostone from the South China Sea, and a bivalve mollusk *Atrina rigid*. The limestone and
45 dolostone samples consist of pure calcite and dolomite, respectively. Their sampling information and
46 elemental concentrations have been reported in the literature.^{44,45} The bivalve was collected by Prof. Joseph
47 G. Carter from Sanibel, Florida. About 62 g calcite shell was cleaned by ultra pure water (Milli-Q) before
48 being dried and then powdered by a Spex Certiprep[®] ball mill at the University of North Carolina at Chapel
49 Hill (UNC-CH). We also used three certified carbonate reference materials: a limestone standard (NIST
50 SRM 1d) was obtained from the National Institute of Standards and Technology (NIST), while a coral (JCp-
51
52
53
54
55
56
57
58
59
60

1
2
3 1) and a dolostone standard (JDo-1) were obtained from the Geological Survey of Japan (GSJ). One basalt
4 standard (BHVO-2) was also included to monitor the accuracy of the K isotope analysis.
5

6
7 In addition, we mixed single-element ICP-MS standards (Inorganic VenturesTM, USA) to prepare a
8 synthetic solution, containing 7460 µg/g Na, 4943 µg/g Mg, 4675 µg/g K, 4497 µg/g Ca, 1924 µg/g Ti, 96
9 µg/g V, 75 µg/g Cr, 1019 µg/g Fe, and 256 µg/g Rb in 2% (v/v) HNO₃. The elemental composition was
10 determined by taking the maximum concentration of each element in the residues of the studied carbonates
11 after the first column. The mixed solution aims to emulate the matrix residue of carbonate samples after the
12 first column and to test the separation of the second column.
13
14
15

16 17 **2.2 Sample preparation**

18
19 To achieve total dissolution, ~50–250 mg of carbonate powder samples were pretreated with 30% H₂O₂
20 (Optima grade, Fisher) to remove organics before being digested through a three-step protocol: the samples
21 were first digested with an HF-HNO₃ (3:1, v/v) mixture on a hot plate at ~150 °C overnight. After the
22 samples were evaporated to dryness, the residues were then treated with *aqua regia* on a hot plate at ~150 °C
23 to achieve total dissolution. Finally, the samples were dried down and redissolved in 2 mL 0.7 M HNO₃ for
24 chromatography. Apart from the carbonates, 1 mL synthetic solution was evaporated and redissolved by
25 acid before being loaded onto the second column. All sample preparation was performed using SavillexTM
26 Teflon beakers in a class 100 laminar flow exhaust hood (AirClean[®] 600 PCR workstation) at the Plasma
27 Spectrometry (PMS) Laboratory at UNC-CH.
28
29
30
31
32
33

34 35 **2.3 Cation exchange chromatography**

36 A dual-column chromatography was optimized for the purification of K from carbonate matrices. The first
37 column was used to separate K from the major carbonate matrix, and the second smaller column was able
38 to further remove residual impurities from K.
39
40

41 We optimized the loading amount and calibrated the K elution range for the first column of Chen *et al.*⁴³
42 The columns were prepared using Bio-RadTM Econo-Pac columns (1.5 cm ID, polypropylene) packed with
43 17 mL Bio-RadTM precleaned AG50W-X8 (100–200 mesh) resin. Columns were first cleaned with 100 mL
44 6 M double-distilled HCl to remove impurities and conditioned with 60 mL 0.7 M HNO₃. Then various
45 amounts of the KL Calcite and SCS Dolomite covering a wide spectrum of marine carbonate matrices
46 (**Table 2**) were loaded onto the columns and eluted using 0.7 M HNO₃. Each 5–10 mL eluent was collected
47 continuously. A total of 190 mL was collected for each sample. All elution cuts were evaporated and
48 dissolved in 2% (v/v) HNO₃ for ICP-MS analysis.
49
50
51
52
53
54
55
56
57
58
59
60

1
2
3 A suite of experiments was carried out using a synthetic solution to optimize chromatographic parameters
4 for the second column, which is built on a customized polypropylene column (0.8 cm ID). **Table 3** gives a
5 summary of column parameters tested, including resin type, column length (aspect ratio), acid type, and
6 acid molarity. In general, the column was pre-cleaned with 20 mL 6 M HCl and 20 mL Milli-Q water before
7 being conditioned with acid. After conditioning, 1 mL synthetic solution was loaded onto the column, and
8 eluents were collected per 5 mL for elemental analysis until K was eluted out completely. Acids used for
9 conditioning, loading, and elution were kept the same. A parallel study was also performed using the same
10 synthetic solution on the second column by Chen *et al.*⁴³ for comparison. The K separation of the optimized
11 second column was further tested by certified references and natural carbonate samples (**Table 4**). We
12 selected ~30–100 mg high-K samples (i.e., NIST SRM 1d, BHVO-2) with K ranging from ~37 to 179 µg
13 to evaluate the influence of the amount of loaded K and other matrix cations on the separation of our method.
14 The rest low-K carbonates weighing within the optimal loading amount of the first column (100–150 mg)
15 were also investigated aiming to obtain enough K (> 1 µg) for isotopic analysis. These samples were passed
16 through the first column before being loaded onto the second column to obtain the calibration curves. K
17 recoveries were monitored throughout the procedure.

18
19
20 Finally, we applied the developed dual-column protocol (**Table 5**) to isolate K from four certified references
21 NIST SRM 1d, JCp-1, JDo-1, BHVO-2, and one in-house South China Sea dolostone sample. We also
22 tested the procedural blanks 4 times using four different columns following the same procedure as the
23 reference. The method is detailed as follows. After loading the sample on the first column, 75 mL of 0.7 M
24 HNO₃ was added to elute the matrix elements, followed by another 5 mL 0.7 M HNO₃ collected into a 7
25 mL Savillex™ beaker as the pre-cut. K was eluted by adding 80 mL 0.7 M HNO₃ and then 5 mL post-cut
26 was collected. The K collection was evaporated, redissolved in 0.4 M HNO₃, and then loaded onto the
27 second column. K fraction was collected between 60–100 mL. 5 mL pre-cut and post-cut were collected
28 before and after the K fraction, respectively. All pre-cuts and post-cuts from two steps of the column, as
29 well as the K fraction of each sample, were measured with a Q-ICP-MS (Agilent™ 7900) to monitor the
30 recovery. The recovered K was dried down and redissolved with 2% (v/v) HNO₃ for isotopic analysis using
31 a Sapphire™ MC-ICP-MS.

32 33 34 **2.4 Instrumental analysis**

35
36
37 To obtain elution curves for both first and second columns, the elution cuts were analyzed using an
38 Agilent™ 7900 quadrupole ICP-MS (Q-ICP-MS) at the PMS Lab, UNC-CH. Samples in 2% (v/v) HNO₃
39 were calibrated using matrix-matched multi-element standards before being measured under helium cell
40 mode to reduce interferences. An internal standard solution containing 100 ng/g of Be, Ge, In, and Bi was
41 used to correct for the instrumental drift. A river water standard SLRS-6 obtained from the National
42
43
44
45
46
47
48
49
50
51
52
53
54
55
56
57
58
59
60

1
2
3 Research Council of Canada was measured routinely, yielding a long-term accuracy of ~5% for major
4 elements, compared with certified values and the GEOREM database.⁴⁶
5
6

7 All K isotopic analyses in this study were conducted following the method by Chen *et al.*⁴⁷ using a Nu
8 Instruments Sapphire™ MC-ICP-MS (SP004) in the Novel Isotopes in Climate, Environment, and Rocks
9 (NICER) Laboratory at the Lamont-Doherty Earth Observatory, Columbia University. Potassium isotope
10 ratios (⁴¹K/³⁹K) were determined using the standard-sample bracketing method. Samples and standard NIST
11 SRM 3141a were diluted to 150 ± 1.5 ppb K solutions in 2% (v/v) HNO₃ for analysis. K solutions were
12 introduced into a “dry plasma” through the Apex Omega desolvating nebulizer (ESI™), and ³⁹K and ⁴¹K
13 signals were measured by Faraday cups equipped with 10¹⁰ Ω and 10¹¹ Ω resistors, respectively. The
14 Sapphire™ MC-ICP-MS is equipped with a collision cell where He and H₂ work as collision gas and
15 reaction gas respectively, to minimize the isobaric interferences of Ar⁺ and ArH⁺, so that potassium isotope
16 signals can be directly measured on the peak center with a 1300 W RF power in low resolution mode. Prior
17 to each analysis, a 20 s on-peak acid blank was measured and subtracted from the analyte signal, and a
18 typical signal for 150 ppb ³⁹K could reach as high as ~165 V. Mass 40 was constantly monitored for Ca
19 level as ⁴⁰CaH⁺ directly interferes with ⁴¹K⁺. Each analysis consisted of 45 cycles of 4 s integrations and
20 took ~100 ng K. Analyses were repeated at least four times for all samples in this study. Their K isotope
21 data are reported in δ⁴¹K relative to the standard NIST SRM 3141a:
22
23
24
25
26
27
28
29
30

31
32
33
34
35
36
37
38
39

$$\delta^{41}\text{K}(\text{‰}) = \left\{ \frac{\left(\frac{^{41}\text{K}}{^{39}\text{K}} \right)_{\text{sample}}}{\left(\frac{^{41}\text{K}}{^{39}\text{K}} \right)_{\text{SRM3141a}}} - 1 \right\} \times 1000$$

40 The long-term external reproducibility of better than 0.07‰ (2SD) was obtained based on the replicate
41 analyses of a seawater sample.⁴⁷
42
43

44 3. Results and discussion

45 3.1 Optimization of the first column

46 The first column is designed to separate K from major elements (*e.g.*, Na, Al, Mg, Ca) in carbonate samples.
47 Its original protocol by Chen *et al.*⁴³ has been extensively applied to extract K from ~10–100 mg silicates
48 for isotopic analysis.^{12,13,17,20,48} However, it is not suitable for low-K carbonates due to remarkably high Ca
49 and/or Mg in the matrix. Such matrices will cause significant elemental peak shifts, leading to unsatisfactory
50 K separation.
51
52
53
54
55
56
57
58
59
60

1
2
3 Elution profiles of Na, Mg, K, and Ca obtained for the first column calibrated with a KL calcite and a SCS
4 dolostone are listed in **Table 2**, and shown in **Fig. 1**. We note here that elution profiles are shown by the
5 bubbles instead of the elution curves in percentage since they can provide more accurate elemental elution
6 ranges (see discussion in Section 3.2). For all the samples tested, increasing the column load shifts K elution
7 peaks leftwards and increase the K elution width. K is consistently eluted from 80 to 160 mL when the
8 column is loaded with dolomite less than 150 mg, whereas a small amount of K can be observed in the cuts
9 prior to 80 mL with a larger loading amount. A similar K elution pattern is also observed in 200 mg calcite,
10 where K is collected in elution cuts before 80 mL and after 160 mL.
11
12
13
14
15

16 High Mg concentrations in carbonates especially in dolostones make it difficult to separate K from Mg.
17 Calibration results show that higher loading cation quantity leads to more Mg breakthroughs into K
18 fractions (**Fig. 1**), and satisfactory K separation can only be achieved with less than 150 mg carbonate.
19 Overlaps between Mg and K observed for 200 mg and 250 mg dolomite yield Mg/K ratios of 646 (ng/ng)
20 and 7283 (ng/ng), respectively, in K fractions. Such an amount of Mg necessitates repeated columns, which,
21 however, may introduce non-trivial contamination from the eluent given the low K abundance in carbonate.
22 The presence of excessive Mg may also cause a matrix effect that results in inaccurate K concentration
23 measurements on Q-ICP-MS.
24
25
26
27
28
29

30 Calcium can be completely separated from K using the first column, regardless of the loading amount and
31 mineralogy. This is important because K isotope measurement can be significantly shifted by CaH^+ .⁴⁷ In
32 contrast, breakthroughs of Na into K fractions are unavoidable during the first column procedure. Similar
33 distribution coefficients of Na and K decrease the separation effectiveness of the first column.⁴⁹
34
35
36

37 In summary, 100–150 mg carbonates are preferred for the first column for their consistent K elution range
38 and effective separation from most matrices. K recoveries after the column optimization were nearly 100%
39 ensuring no on-column isotopic fractionation. Nevertheless, the application of the first column cannot
40 achieve complete K isolation in observance of the small amount of residual Na and Mg, as well as trace
41 elements including Rb, V, and Ti collected in the K fraction. Hence, an additional second column is needed
42 for further purification. All samples used for the subsequent column development were kept under 150 mg.
43
44
45
46

47 **3.2 Development of the second column**

48

49 Bio-Rad™ AG50W-X8 resin (100–200 mesh) with an 8% crosslink is commonly used in existing K
50 chromatographic procedures (**Table 1**). AG50W-X12 (200–400 mesh) resin is expected to have a larger
51 loading capacity and better separation resolution due to its larger crosslink rate (12%) and total surface
52 area.⁵⁰ Therefore, both resins were loaded in an identical column (0.8 cm ID), and calibrated using the same
53 synthetic solution (**Table 3**). Calibration results present two advantages of X8 resin over X12 resin (**Fig. 2**,
54
55
56
57
58
59
60

1
2
3) First, the column packed with X8 resin has a shorter elution duration of K separation using the same
4 acid. For example, a 60 mL K peak gap is found between X8 (25–65 mL, **Fig. 2f**) and X12 resin (85–135
5 mL, **Fig. 3b**) using 0.7 M HNO₃ as the eluent. A similar gap can also be found for 1 M HCl, where X8 and
6 X12 resins have K peaks ranging from 15 to 50 mL and 50 to 90 mL (**Table 3**), respectively. Second, the
7 application of X12 resin is limited by V and Ti overlapping with K (**Fig. 3**). Although X12 resin eluted by
8 0.5 M HNO₃ seems to sufficiently isolate K (**Fig. 3a**), the K retention time is more than 12 h.
9
10

11
12
13 Elution profiles of the mixed solution were obtained for X8 resin with HNO₃ and HCl (**Fig. 2**). For both
14 acids, less concentrated acid can spread out the elemental peaks, thereby co-elution matrix can be
15 effectively eliminated. Among all the elution acids, 0.4 M HNO₃ is preferred due to the following reasons:
16 1) No Na, V, Ti, Mg, and Ca were collected in the K fraction; and 2) K elution range is 60–100 mL, the
17 separation work can be finished in about 8 h at the elution rate of 0.2 mL/min. A previous study suggested
18 using a larger aspect ratio column to improve the separation efficiency.⁵¹ However, such improvement is
19 negligible in the long column (17 cm) tested in this study (**Fig. 2c, e**) and a significantly longer retention
20 time is present.
21
22

23
24
25 We also loaded 1 mL mixed solution onto the second column by Chen *et al.*⁴³ for comparison. The results
26 are shown by both “bubbles” and elution curves (**Fig. 4**). We have found that the overlap between elements
27 in the bubble figure is sometimes unidentifiable in the elution curves, because the small tails at both ends
28 of the elution curves could be shaded by the major peak. Here we note that although elution curves can
29 provide the elution order and the curve tailing, they cannot provide the accurate elution range and the
30 separation effectiveness, especially for columns loaded with heavy matrix materials. The elution curves of
31 our second column are consistent with the bubble figure that no Na was collected in the K fraction (**Fig.**
32 **4a**). However, Na breakthrough into the K fraction can be observed in the second column by Chen *et al.*⁴³,
33 even though elution curves show no overlap (**Fig. 4b**). Compared with Na, Rb cannot be completely
34 removed using both columns. Yet Rb is not problematic for our column due to its low content in natural
35 carbonates (see discussion below).
36
37

38
39
40 Potassium was chromatographically isolated from certified references and natural carbonate samples
41 (**Table 4**). First, the samples were passed through the first column, during which no K loss was found. The
42 K cuts were then loaded onto the second column to get the calibration results (**Fig. 5**). With loaded K⁺
43 ranging from 1.7 to 179.1 μg, K peaks constantly fall into 60–100 mL, consistent with the elution range
44 obtained using the synthetic solution. In addition, a 5–20 mL elution gap between Na and K ensures the
45 total K recovery without any Na. And for all the samples tested, Rb/K was always less than 0.3% after the
46 columns (**Table 4**). Such impurities will not compromise the accuracy of K isotope measurement,⁴⁷ so we
47 do not need to repeat this column. Furthermore, our newly developed dual-column method yields
48
49
50
51
52
53
54
55
56
57
58
59
60

satisfactory K recovery of nearly 100% (**Table 4**) without any isotopic fractionation during the column chemistry.

The average of the four total procedure blanks for the entire K purification process is 29.5 ± 4.4 ng (2SD; $n=4$), which is about 9 times lower than that of Chen *et al.*⁴³ (0.26 ± 0.15 μg , 2SD, $n=7$). In our study, KL calcite has a minimum K of 1.73 μg , yielding a sample/blank ratio of 59. Assuming the blank has the $\delta^{41}\text{K}$ value of -1.31‰ ,⁴³ the blank will introduce an error of $\sim 0.02\text{‰}$, which is below the analytical uncertainty of K isotope measurement. Therefore, the blank is negligible for all samples tested in this study. The whole experimental process generally takes 2 days, including all the column and evaporation steps. Although our method does not significantly reduce the experimental time, our method is more efficient than existing dual-column protocols because their protocols need repeated separation for low-K carbonates either to eliminate matrices or to obtain enough K (i.e., 1 μg) for isotopic analysis using MC-ICP-MS.²⁷

3.3 The K isotope composition of reference materials

We report potassium isotope compositions of the following materials: BHVO-2 (basalt), NIST SRM 1d (limestone), JCp-1 (coral), JDo-1 (dolostone), and SCS dolostone to evaluate the reproducibility of our newly developed chromatographic method and to facilitate inter-laboratory comparison (**Table 6**). Basalt BHVO-2 is one of the most extensively used geologic standards. Therefore a BHVO-2 sample was processed and analyzed using our method, its K isotope value ($-0.41 \pm 0.03\text{‰}$, $n=6$) is in good agreement with previous studies. This validates the analytical accuracy of this study, and also implies the potential of our method in dealing with other low-K samples beyond carbonate (e.g., ultramafic rocks). The K isotope compositions of two NIST SRM 1d are $-0.60 \pm 0.02\text{‰}$ (2SD, $n=6$) and $-0.57 \pm 0.04\text{‰}$ (2SD, $n=4$), respectively. The results are consistent with previously published data ($-0.65 \pm 0.09\text{‰}$, 95% C.I., $n=8$; Li *et al.*³³). The $\delta^{41}\text{K}$ value of the coral aragonite standard JCp-1 (-0.31 ± 0.02 , 2SD, $n=6$) is lower than the previous values reported by Li *et al.*^{32,33} (**Table 6**). The varied $\delta^{41}\text{K}$ values might reflect the heterogeneity of the reference material, which has been reported for lithium^{52,53} and thorium isotopes⁵⁴. The $\delta^{41}\text{K}$ values of JDo-1 are reported for the first time. Two individual JDo-1 standards yield the same $\delta^{41}\text{K}$ value of $-1.00 \pm 0.01\text{‰}$ (2SD, $n=6$) within our analytical precision. We also report the $\delta^{41}\text{K}$ value of an in-house carbonate sample, South China Sea dolostone. Three individual experiments on one dolostone sample yield indistinguishable K isotope values, proving the robustness of our method in applications on natural carbonate samples.

Conclusion

We present the results of a series of experiments that optimize the dual-column chromatography to purify K for high-precision isotope analysis in carbonate materials using MC-ICP-MS. Our method can isolate K

1
2
3 from 100–150 mg chemically diverse carbonate samples with satisfactory yield (~100%) and negligible
4 total blank (29.5 ± 4.4 ng). Finally, we report K isotope compositions in carbonate reference materials NIST
5 SRM 1d (limestone), JCp-1 (coral), JDo-1 (dolostone), and an in-house dolostone sample, in addition to a
6 common silicate reference BHVO-2 for inter-laboratory comparison. Both NIST SRM 1d and BHVO-2
7 $\delta^{41}\text{K}$ results agree well with published data, whereas a lower JCp-1 $\delta^{41}\text{K}$ value may be caused by the
8 heterogeneity of this reference material. Here we first report the $\delta^{41}\text{K}$ value of -1.00‰ in a dolomite
9 standard, JDo-1. The developed K purification method facilitates the application of K isotopes in marine
10 carbonates for future geochemical and paleoceanographic research.
11
12
13
14
15

16 **Author Contributions**

17
18
19 X.-K. Wang was responsible for the conceptualization, investigation, and writing the original draft. X.-M.
20 Liu is responsible for the conceptualization, funding acquisition, supervision, and writing, reviewing, and
21 editing of the manuscript. H. Chen is responsible for the investigation, manuscript writing, reviewing, and
22 editing.
23
24
25

26 **Acknowledgments**

27
28 The authors acknowledge the funding support from the NSF Career Award (EAR-1848153) to X.-M. Liu,
29 the Martin Research Fellowship from the University of North Carolina at Chapel Hill to X.-K. Wang. We
30 thank Joseph G. Carter, Cheng Cao, and Xiao-Feng Liu for providing the samples, and Wenshuai Li for
31 helpful discussions and comments on earlier drafts. We also thank two anonymous reviewers for thorough
32 and constructive reviews, and the editor for handling the manuscript.
33
34
35
36
37
38
39
40
41
42
43
44
45
46
47
48
49
50
51
52
53
54
55
56
57
58
59
60

References

- 1 E. D. Goldberg, *J. Chem. Educ.*, 1958, **35**, 113–115.
- 2 J. Sardans and J. Peñuelas, *Glob. Ecol. Biogeogr.*, 2015, **24**, 261–275.
- 3 A. Y. Mulkidjanian, A. Y. Bychkov, D. V. Dibrova, M. Y. Galperin and E. V. Koonin, *Proc. Natl. Acad. Sci. U. S. A.*, 2012, **109**, 820–830.
- 4 M. W. Szczerba, D. T. Britto and H. J. Kronzucker, *J. Plant Physiol.*, 2009, **166**, 447–466.
- 5 W. Li, X.-M. Liu, Y. Hu, F.-Z. Teng, Y.-F. Hu and O. A. Chadwick, *Geoderma*, 2021, **400**, 115219.
- 6 N. J. W. Clipson and D. H. Jennings, *Mycol. Res.*, 1990, **94**, 1017–1022.
- 7 R. L. Rudnick and S. Gao, *Composition of the Continental Crust*, Elsevier Ltd., 2nd Edn., 2013, vol. 4.
- 8 F. Culkin and R. A. Cox, *Deep. Res. Oceanogr. Abstr.*, 1966, **13**, 789–804.
- 9 N. M. Johnson, G. E. Likens, F. H. Bormann and R. S. Pierce, *Geochim. Cosmochim. Acta*, 1968, **32**, 531–545.
- 10 F.-Z. Teng, Y. Hu, J.-L. Ma, G.-J. Wei and R. L. Rudnick, *Geochim. Cosmochim. Acta*, 2020, **278**, 261–271.
- 11 S. Li, W. Li, B. L. Beard, M. E. Raymo, X. Wang, Y. Chen and J. Chen, *Proc. Natl. Acad. Sci. U. S. A.*, 2019, **116**, 8740–8745.
- 12 H. Chen, X.-M. Liu and K. Wang, *Earth Planet. Sci. Lett.*, 2020, **539**, 116192.
- 13 W. Li, X.-M. Liu, K. Wang and P. Koefoed, *Chem. Geol.*, 2021, **568**, 120142.
- 14 P. Michalopoulos and R. C. Aller, *Science*, 1995, **270**, 614–617.
- 15 F. T. Mackenzie and R. M. Garrels, *Am. J. Sci.*, 1966, **264**, 507–525.
- 16 D. P. Santiago Ramos, L. E. Morgan, N. S. Lloyd and J. A. Higgins, *Geochim. Cosmochim. Acta*, 2018, **236**, 99–120.
- 17 W. Li, X.-M. Liu, Y. Hu, F.-Z. Teng and Y. Hu, *Geochim. Cosmochim. Acta*, 2021, **304**, 160–177.
- 18 S. Bloch and J. L. Bischoff, *Geology*, 1979, **7**, 193–196.
- 19 R. Hart, *Earth Planet. Sci. Lett.*, 1970, **9**, 269–279.
- 20 H. Liu, Y.-Y. Xue, G. Zhang, W.-D. Sun, Z. Tian, B. Tuller-Ross and K. Wang (王昆), *Geochim. Cosmochim. Acta*, 2021, **311**, 59–73.
- 21 X.-Y. Zheng, B. L. Beard, M. Neuman, M. F. Fahnstock, J. G. Bryce and C. M. Johnson, *Earth Planet. Sci. Lett.*, 2022, **593**, 117653.
- 22 D. P. Santiago Ramos, L. A. Coogan, J. G. Murphy and J. A. Higgins, *Earth Planet. Sci. Lett.*, 2020, **541**, 116290.
- 23 M. Hille, Y. Hu, T.-Y. Huang and F.-Z. Teng, *Sci. Bull.*, 2019, **64**, 1740–1742.
- 24 K. Wang, H. G. Close, B. Tuller-Ross and H. Chen, *ACS Earth Sp. Chem.*, 2020, **4**, 1010–1017.

- 1
2
3 25 K. Wang and S. B. Jacobsen, *Geochim. Cosmochim. Acta*, 2016, **178**, 223–232.
4
5 26 B. Tuller-Ross, B. Marty, H. Chen, K. A. Kelley, H. Lee and K. Wang, *Geochim. Cosmochim.*
6 *Acta*, 2019, **259**, 144–154.
7
8 27 K. Wang, W. Li, S. Li, Z. Tian, P. Koefoed and X.-Y. Zheng, *Geochemistry*, 2021, **81**, 125786.
9
10 28 X. Zhou, Y. Rosenthal, L. Haynes, W. Si, D. Evans, K.-F. Huang, B. Hönisch and J. Erez,
11 *Geochim. Cosmochim. Acta*, 2021, **305**, 306–322.
12
13 29 Y. Rosenthal, E. A. Boyle and N. Slowey, *Geochim. Cosmochim. Acta*, 1997, **61**, 3633–3643.
14
15 30 X.-M. Liu, L. C. Kah, A. H. Knoll, H. Cui, C. Wang, A. Bekker and R. M. Hazen, *Nat. Commun.*,
16 2021, **12**, 1–7.
17
18 31 H. Jurikova, M. Gutjahr, K. Wallmann, S. Flögel, V. Liebetrau, R. Posenato, L. Angiolini, C.
19 Garbelli, U. Brand, M. Wiedenbeck and A. Eisenhauer, *Nat. Geosci.*, 2020, **13**, 745–750.
20
21 32 W. Li, X.-M. Liu, K. Wang, F. J. Fodrie, T. Yoshimura and Y.-F. Hu, *Geochim. Cosmochim. Acta*,
22 2021, **304**, 364–380.
23
24 33 W. Li, X.-M. Liu, K. Wang, Y. Hu, A. Suzuki and T. Yoshimura, *Earth Planet. Sci. Lett.*, 2022,
25 **581**, 117393.
26
27 34 X.-Y. Zheng, X.-Y. Chen, W. Ding, Y. Zhang, S. Charin and Y. Gérard, *J. Anal. At. Spectrom.*,
28 2022, **37**, 1273–1287.
29
30 35 X. Li, G. Han, Q. Zhang and Z. Miao, *J. Anal. At. Spectrom.*, 2020, **35**, 1330–1339.
31
32 36 X. Li and G. Han, *J. Anal. At. Spectrom.*, 2021, **36**, 676–684.
33
34 37 W. Li, B. L. Beard and S. Li, *J. Anal. At. Spectrom.*, 2016, **31**, 1023–1029.
35
36 38 Y. Hu, X.-Y. Chen, Y.-K. Xu and F.-Z. Teng, *Chem. Geol.*, 2018, **493**, 100–108.
37
38 39 C. Huang, H.-O. Gu, H. Sun, F. Wang and B. Chen, *Spectrochim. Acta - Part B At. Spectrosc.*,
39 2021, **181**, 106232.
40
41 40 R. H. James and M. R. Palmer, *Chem. Geol.*, 2000, **166**, 319–326.
42
43 41 W. Li, X.-M. Liu and L. V. Godfrey, *Geostand. Geoanalytical Res.*, 2019, **43**, 261–276.
44
45 42 M. Humayun and R. N. Clayton, *Geochim. Cosmochim. Acta*, 1995, **59**, 2115–2130.
46
47 43 H. Chen, Z. Tian, B. Tuller-Ross, R. L. Korotev and K. Wang, *J. Anal. At. Spectrom.*, 2019, **34**,
48 160–171.
49
50 44 X.-F. Liu, S. Zhai, X.-K. Wang, X. Liu and X.-M. Liu, *Minerals*, 2022, **12**, 578.
51
52 45 C. Cao, X.-M. Liu, C. P. Bataille and C. Liu, *Chem. Geol.*, 2020, **532**, 119413.
53
54 46 K. P. Jochum, U. Nohl, K. Herwig, E. Lammel, B. Stoll and A. W. Hofmann, *Geostand.*
55 *Geoanalytical Res.*, 2005, **29**, 333–338.
56
57 47 H. Chen, N. J. Saunders, M. Jerram and A. N. Halliday, *Chem. Geol.*, 2021, **578**, 120281.
58
59 48 H. Liu, K. Wang(王昆), W.-D. Sun, Y. Xiao, Y.-Y. Xue and B. Tuller-Ross, *Geochim.*
60 *Cosmochim. Acta*, 2020, **277**, 206–223.

- 1
2
3 49 F. W. E. Strelow, R. Rethemeyer and C. J. C. Bothma, *Anal. Chem.*, 1965, **37**, 106–111.
4
5 50 C. M. Davies, University of Manchester, 2012.
6
7 51 P. A. Sossi, G. P. Halverson, O. Nebel and S. M. Eggins, 2014, **39**, 129–149.
8
9 52 L. Bastian, N. Vigier, S. Reynaud, M. E. Kerros, M. Revel and G. Bayon, *Geostand.*
10 *Geoanalytical Res.*, 2018, **42**, 403–415.
11
12 53 G. Zhu, J. Ma, G. Wei and L. Zhang, *Front. Chem.*, 2020, **8**, DOI:10.3389/fchem.2020.557489.
13
14 54 Y. Watanabe and S. Nakai, *Geochem. J.*, 2006, **40**, 537–541.
15
16 55 E. W. E. Strelow, F. Von and C. H. S. W. Weinert, *Anal. Chim. Acta*, 1970, **50**, 399–405.
17
18 56 W. Li, B. L. Beard and S. Li, *J. Anal. At. Spectrom.*, 2016, **31**, 1023–1029.
19
20 57 L. E. Morgan, D. P. Santiago Ramos, B. Davidheiser-Kroll, J. Faithfull, N. S. Lloyd, R. M. Ellam
21 and J. A. Higgins, *J. Anal. At. Spectrom.*, 2018, **33**, 175–186.
22
23 58 F. Moynier, Y. Hu, K. Wang, Y. Zhao, Y. Gérard, Z. Deng, J. Moureau, W. Li, J. I. Simon and F. -
24 Z. Teng, *Chem. Geol.*, 2021, **571**, 120144.
25
26
27
28
29
30
31
32
33
34
35
36
37
38
39
40
41
42
43
44
45
46
47
48
49
50
51
52
53
54
55
56
57
58
59
60

Figure captions

Fig. 1. Elution profiles for ~100–250 mg KL Cal and SCS Dol via the first column of Chen *et al.*⁴³ Elution profiles are shown by conceptual bubbles. Two ends of a bubble indicate the elution fraction range.

Fig. 2. Elution curves for the synthetic solution with different eluents on AG50X8 resin (100–200 mesh). L indicates a longer column (17 cm).

Fig. 3. Elution curves for the synthetic solution with different eluents on AG50X12 resin (200–400 mesh). L indicates a longer column (17 cm).

Fig. 4. Elution profiles of the synthetic solution using (a) the second column developed in this study and (b) the second column of Chen *et al.*⁴³ are shown by elution curves (upper panel) and conceptual bubbles (lower panel). Two ends of the bubble indicate the accurate elution range of the cation.

Fig. 5. Elution curves of natural carbonates and reference materials via the second column separation after the first column purification. The K elution range (bracketed by the grey dashed line) is 60–100 mL. Na is absent in K fractions, Rb/K is less than 0.3%.

Table 1. Potassium ion-exchange separation procedure comparison (modified after Wang *et al.*²⁷).

	Strelow <i>et al.</i> ⁵⁵	Humayun and Clayton ⁴²	Wang and Jacobson ²⁵	Li <i>et al.</i> ⁵⁶	Morgan <i>et al.</i> ⁵⁷	Hu <i>et al.</i> ³⁸	Chen <i>et al.</i> ⁴³	Li <i>et al.</i> ³⁵	Chen <i>et al.</i> ⁴⁷	Huang <i>et al.</i> ³⁹
Number of columns	1	1	1	2		1	2	1	1	1
Sample weight	~1 g	~1 g	~10–50 mg	10–50 mg	~20 mg		~10–100 mg	~50 mg	<20 mg	10–20 mg
Resin	Bio-Rad AG50W-X8 (200–400 mesh)	Bio-Rad AG50W-X8 (100–200 mesh)	Bio-Rad AG50W-X8 (100–200 mesh)	Bio-Rad AG50W-X12 (100–200 mesh)	Dionex CS-16 cation exchange column	Bio-Rad AG50W-X8 (200–400 mesh)	Bio-Rad AG50W-X8 (100–200 mesh)	Bio-Rad AG50W-X8 (200–400 mesh)	Bio-Rad AG50W-X8 (200–400 mesh)	Bio-Rad AG50W-X8 (200–400 mesh)
Column type	Borosilicate glass	Pyrex or quartz	Quartz	Quartz		Bio-Rad Poly-Prep polyethylene column	Bio-Rad Poly-Prep Econo-Pac polyethylene column	Savillex PFA micro-column	Bio-Rad Poly-Prep polyethylene column	Quartz
Diameter	2.5 cm	2.2 cm	1 cm	0.4 cm		0.8 cm	1.5 cm	4 mm		7 mm
Resin volume	90 mL	90 mL	13 mL	1 mL		2 mL	17 mL	2.3 mL	2 mL	2.7 mL
Cleaning	3 M HNO ₃	4 M HNO ₃ or 6 M HCl	4 M HCl	4.5 M HNO ₃		6 M HCl + water + 1 M HNO ₃	6 M HCl	6 M HCl + water	6 M HCl	6 M HCl + water
Max capacity* (mEq)	153	153	22.1	2.1		3.4	28.9	3.9	3.4	4.6
Eluting	0.5 M HNO ₃	0.5 M HNO ₃	0.5 M HNO ₃	1.5 M HNO ₃	0.2% HNO ₃	0.5 M HNO ₃	0.7 M HNO ₃	2 M HCl + 0.1 M Hf	0.45 M HCl	0.5 M HNO ₃
Potassium fraction	600–850 mL	700–1000 mL	180–340 mL	5–17 mL		14–36 mL	88–195 mL	12–22 mL	20–45 mL	25–49 mL
Recovery		≥ 99.8	> 99%	99.4 ± 2.1%			> 99%	99.5 ± 0.6%	> 99%	
Blank	0.5–1 µg	0.2%	0.82 µg	3–8 ng	0.06–1.06%		0.26 ± 0.15 µg	<10 ng	0.13 µg	10 ng

*Bio-Rad AG50W-X8 and X12 resins have ion exchange capacity of 1.7 and 2.1 mEq/mL, respectively.

Table 2. Experimental design for the optimization of the first column.

Sample name	Sample weight (mg)	Cation load* (mEq)	Mg ²⁺ mass load (mg)	Ca ²⁺ mass load (mg)	K ⁺ mass load (ng)
SCS Dol	106.6	2.31	10.97	21.44	2669
	150.9	3.27	15.53	30.35	3779
	203.1	4.41	20.90	40.85	5086
	253.5	5.50	26.09	50.99	6348
KL Cal	106.6	2.13	0.25	43.06	1604
	207.0	4.14	0.49	83.63	3115

*Cation load has been calculated assuming all samples are pure carbonates.

Table 3. Parameters of the second columns and K elution ranges.

Resin	Column length (cm)	Elution acid	K fraction (mL)
AG50W-X8 (100–200 mesh)	13	0.3 M HNO ₃	80–140
	13	0.4 M HNO ₃	60–100
	17	0.4 M HNO ₃	65–105
	13	0.5 M HNO ₃	45–85
	17	0.5 M HNO ₃	50–95
	13	0.7 M HNO ₃	25–65
	13	1.0 M HNO ₃	15–45
	13	0.5 M HCl	40–90
	13	1.0 M HCl	15–50
	AG50W-X12 (200–400 mesh)	13	0.5 M HNO ₃
13		0.7 M HNO ₃	85–135
13		1.0 M HNO ₃	50–85
13		0.5 M HCl	125–*
13		1.0 M HCl	50–90

*Potassium was not totally washed out when the experiment stopped.

Table 4. Experimental design and results for the second column.

Sample type	Sample name	Sample weight (mg)	K concentration (µg/g)	K ⁺ mass load (µg)	K elution range (mL)	K recovery (%)	Rb/K (%)
Limestone	NIST SRM 1d (1)	31.6	1174.5	37.1	65–100	100.0	0.10
	NIST SRM 1d (2)	40.9		48.0	60–100	100.0	0.18
	NIST SRM 1d (3)	47.9		56.3	60–100	100.0	0.29
	NIST SRM 1d (4)	105.6		124.0	60–100	100.0	0.27
	KL Cal	115.0	15.1	1.7	65–100	99.7	0.20
Aragonite	In-house Bivalve	122.7	100.4	12.3	60–90	100.0	0.03
	JCp-1	107.9	188.7	20.4	65–95	100.0	0.07
Dolostone	SCS Dol	108.6	25.1	2.7	65–95	100.0	0.09
	JDo-1	109.1	20.9	2.3	65–90	100.0	0.24
Basalt	BHVO-2	39.4	4545.3	179.1	60–100	100.0	0.05

Table 5. Overview of the developed K isotope chromatographic procedure.

First column purification		
17 mL Bio-Rad AG50W-X8 (100–200 mesh) in Bio-Rad Econo-Pac column (1.5 cm ID)		
Step	Solution	Volume (mL)
Cleaning	6 M HCl	100
Conditioning		60
Loading sample		2
Matrix elution	0.7 M HNO ₃	75
Pre-cut 1		5
K Collection		80
Post-cut 1		5
Second column purification step		
6.5 mL Bio-Rad AG50W-X8 (100–200 mesh) in customized polypropylene column (0.8 cm ID)		
Step	Solution	Volume (mL)
Cleaning	6 M HCl	20
	Milli-Q water	20
Conditioning		10
Loading sample		1
Matrix elution	0.4 M HNO ₃	55
Pre-cut 2		5
K Collection		40
Post-cut 2		5

Table 6. K isotope compositions in certified reference materials.

Sample name	Sample type	$\delta^{41}\text{K}$	2SD	N	Data source
BHVO-2	Basalt	-0.50	0.19	4	Li et al. ³⁷
		-0.43	0.06	5	Hu et al. ³⁸
		-0.46	0.04 (2SE)	13	Chen et al. ⁴³
		-0.47	0.03 (2SE)	79	Chen et al. ¹²
		-0.40	0.04	6	Li et al. ³⁵
		-0.48	0.04	7	Li et al. ¹⁷
		-0.47	0.03	26	Chen et al. ⁴⁷
		-0.434	0.04	11	Moynier et al. ⁵⁸
NIST SRM 1c	Limestone	-0.41	0.03	6	This study
		-0.58	0.03 (95% C.I.)	14	Chen et al. ⁴³
NIST SRM 1d	Limestone	-0.65	0.09 (95% C.I.)	8	Li et al. ³³
		-0.60	0.02	6	This study
JCp-1	Aragonite	-0.57	0.04	4	This study
		-0.20	0.07 (95% C.I.)	-	Li et al. ³²
JDo-1	Dolostone	-0.10	0.10 (95% C.I.)	8	Li et al. ³³
		-0.31	0.02	6	This study
JDo-1	Dolostone	-1.00	0.01	6	This study
		-1.00	0.01	6	This study
SCS Dol	Dolostone	-0.49	0.02	4	This study
		-0.48	0.03	4	This study
		-0.50	0.01	6	This study

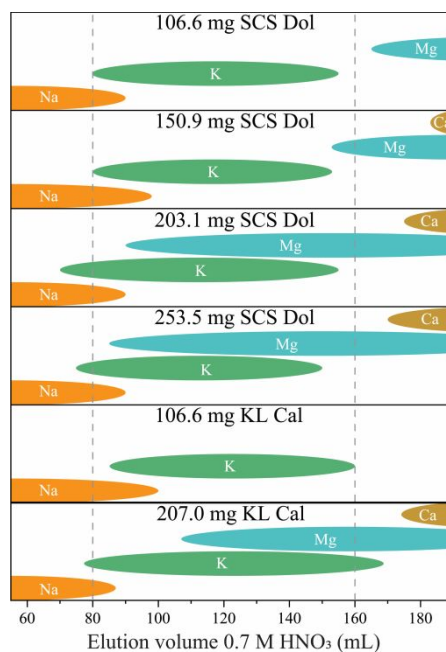
Fig. 1

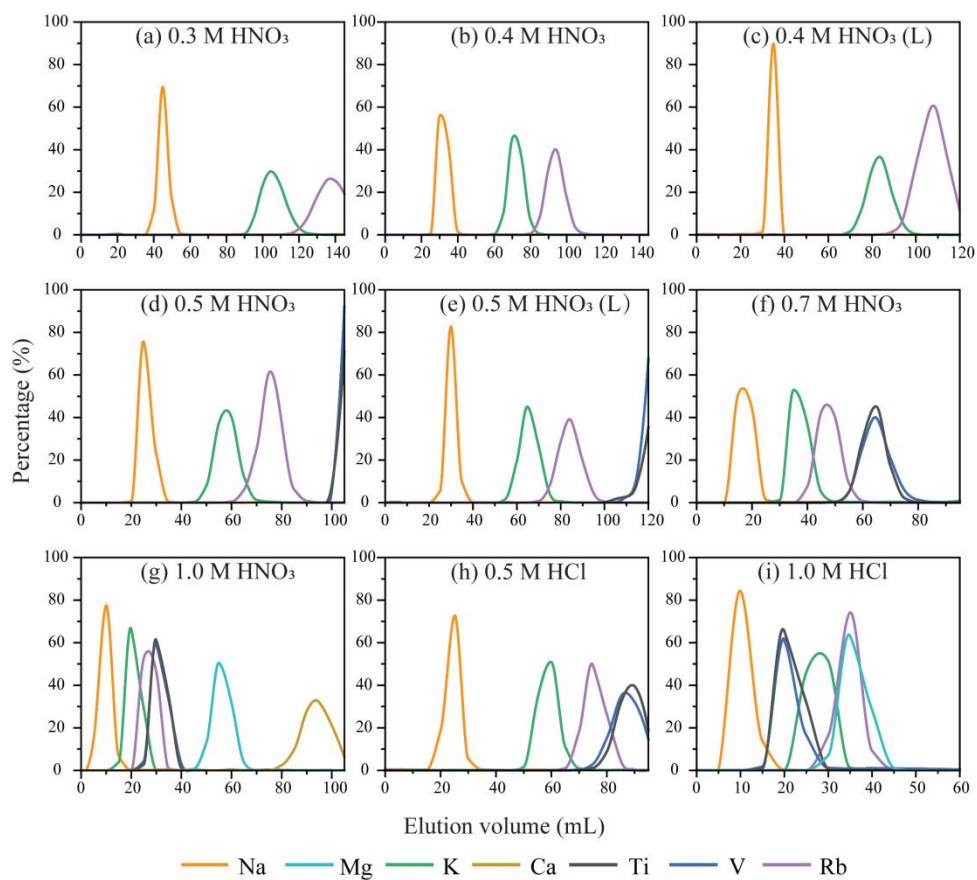
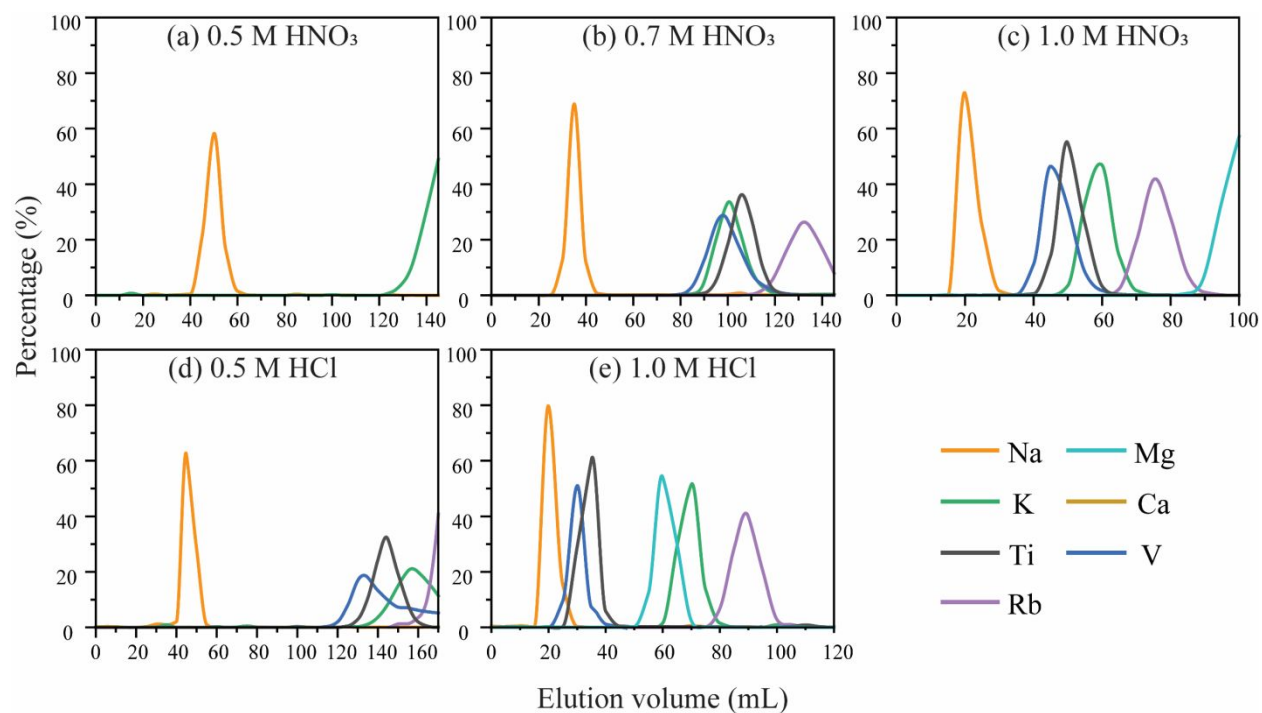
Fig. 2**Fig. 3**

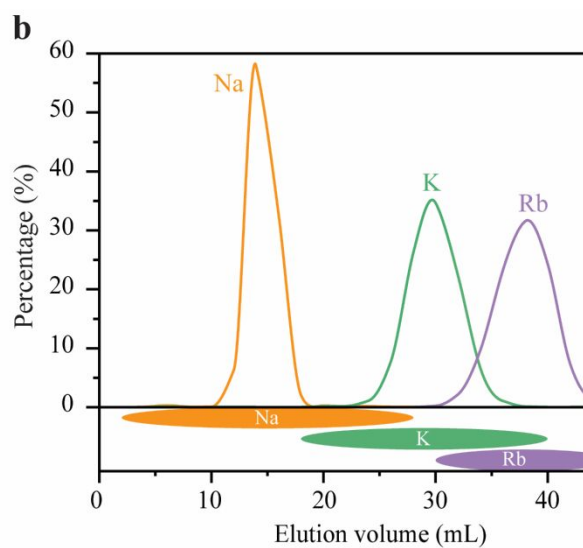
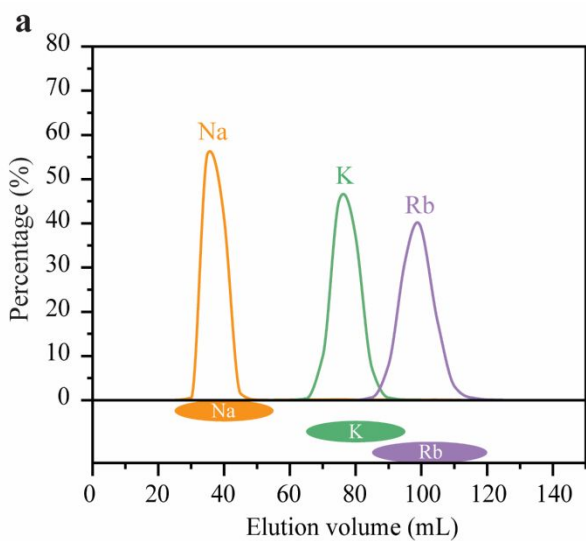
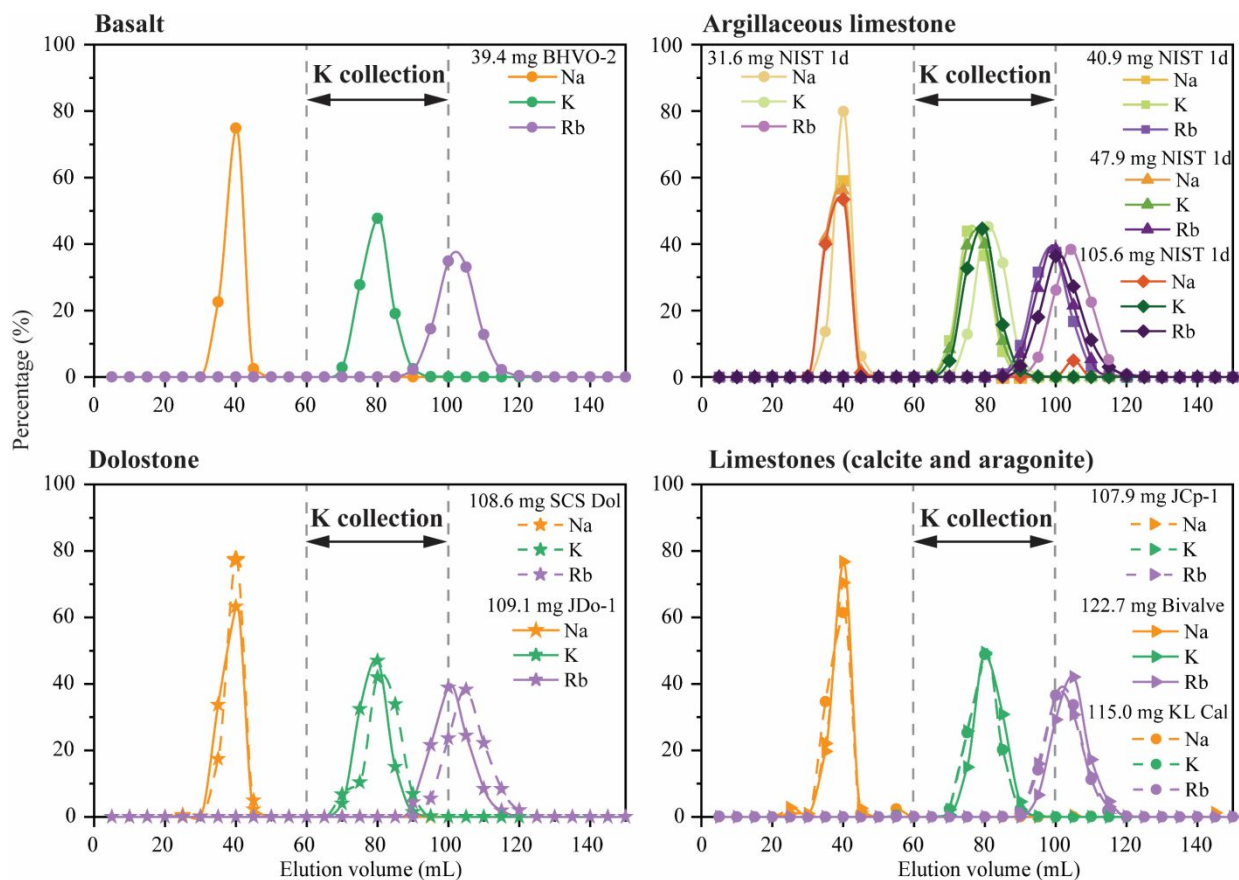
Fig. 4

Fig. 5



1
2
3
4
5
6
7
8
9
10
11
12
13
14
15
16
17
18
19
20
21
22
23
24
25
26
27
28
29
30
31
32
33
34
35
36
37
38
39
40
41
42
43
44
45
46
47
48
49
50
51
52
53
54
55
56
57
58
59
60